# Air Gap Length and Maximum and Minimum Inductance of A Double-Salient Reluctance Machine (DSRM) using The Developed Analytical Algorithm

Enesi Asizehi Yahaya[1], Ajah Victor[2], Emenike Chinedozi Ejiogu[3]

[1]Department of Electrical Engineering, Federal University of Technology, Minna, Nigeria
[2.3]Department of Electrical Engineering, University of Nigeria, Nsukka
[3]Department of Electrical and Electronic Engineering Science, University of Johannesburg, South Africa
[3]Africa Centre of Excellence for Sustainable Power and Energy Development (ACE-SPED), University of Nigeria, Nsukka
[3]Laboratory of Industrial Electronics, Power Devices and New Energy Systems (LIEPNES), University of Nigeria, Nsukka
enesi.asizehi@futminna.edu.ng, victor.ajah.88556@unn.edu.ng, emenike.ejiogu@unn.edu.ng

*Abstract:* In this paper an algorithm is developed to predict the maximum and minimum inductance of an optimized pole arc of a fabricated double salient reluctance machine (DSRM). The developed analytical algorithm investigates the air gap length at the maximum and minimum inductances. These are achieved through the machine rotor pole arc, stator pole arc, bore diameter, back iron thickness, rotor yoke thickness, stack length, and rotor pole diameter. The validity of the newly developed analytical procedures for predicting the maximum and minimum inductances was evaluated using the measurements obtained from the machine prototype. There was a good correlation between the analytical and experimental results. Inductances and air gap lengths of 2/2 DSRM of equal stator and rotor pole width and stator pole width greater than the rotor pole width were investigated and analyzed using the developed algorithm. A second existing DSRM with different numbers of stator and rotor poles whose inductances have been known and compared with finite element analysis (FEA) is chosen to verify the algorithm developed. The 2/2 DSRM's potential to sustain oscillation during energy conversion from mechanical energy to electrical energy is investigated.

*Keywords*: Maximum and minimum inductance, Double salient reluctance machine, Developed analytical algorithm, Experimental results, Finite element analysis, Oscillation

## 1. Introduction

Machines that exhibit double salient structures are switched reluctance machines, permanent magnet machines, hybrid machines and variable stepper motor machines. The maximum and minimum inductance of switched reluctance machines with reference to rotor positions are investigated analytically in [1]–[4]. In [5], the discussion is om the unaligned inductance and saliency ratio when choosing the design ratios for switched reluctance machine design. The applications of switched reluctance machines as motors are found in [6]-[10] and as generator in [11] - [13]. The electromagnetic calculation of a 4/2 doubly salient machine was computed using winding function analysis in [14].

The size of the air gap determines the performance of the electromechanical devices in [15]. The air gap modeling and experimental evaluation are discussed in [16] and [17]. The air gap length is a factor that determines the loss of the magnetic flux between the rotor and stator circuits. Increasing the air gap leads to a corresponding increase in reluctance, flux fringing, and vice versa [18]. A small air gap results in low reluctance and high magnetic flux. These characteristics make the machine more efficient with higher power, as discussed in [19] and [20]. A large air gap length is required in a synchronous machine to decrease leakage reactance, increase the load capacity, improve the cooling, reduce noise, and decrease the unbalanced magnetic pull owing to non-uniform air gaps in the shortest air gap [21].

Received: November 16th, 2021. Accepted: January 11st, 2022
DOI: 10.15676/ijeei.2022.14.1.1

Many techniques have been proposed for measuring inductances. The calculation of inductance and torque of a synchronous reluctance machine with an axially laminated anisotropic rotor using a winding theory was determined in [22]. The authors in [23] used winding function analysis and two-dimensional finite element analysis to calculate the electromagnetic torque and inductances of a synchronous reluctance machine under linear conditions. An accurate method for determining winding inductances of a two-phase stator winding is presented in [24]. The inductance is obtained using the finite element method in [25].

The double salient reluctance machine exhibits saliency in both the rotor and stator cores. The air gap separates the rotor and the stator core. The salient rotor poles do not have windings, whereas the salient stator poles have concentrated coils. A 2.20 kW of 230 V is designed and fabricated with 16 SWG wounds around the stator pole. This is a special salient machine, with the number of stator poles equal to the number of rotor poles. Initially, analytical expressions are developed to predict the air gap lengths, maximum inductance (Lmax), and minimum inductance (Lmin) of the machine. The DSRM is further subjected to a laboratory investigation of its inductance. The proposed analytical algorithm developed is compared to the laboratory results for validation.

## 2. Developed Analytical Algorithm

The novel approach is used to develop an analytical algorithm for predicting 2/2 DSRM air gap lengths and their inductances. The angles subtended by the rotor pole and stator pole at the edges, bore radius Rsp, and rotor pole radius Rrp are shown in Figure. 1. In this DSRM the rotor width is larger than the stator width. The air gap length when the stator and rotor pole are in aligned position is investigated, leading to the prediction of the maximum and minimum inductances.

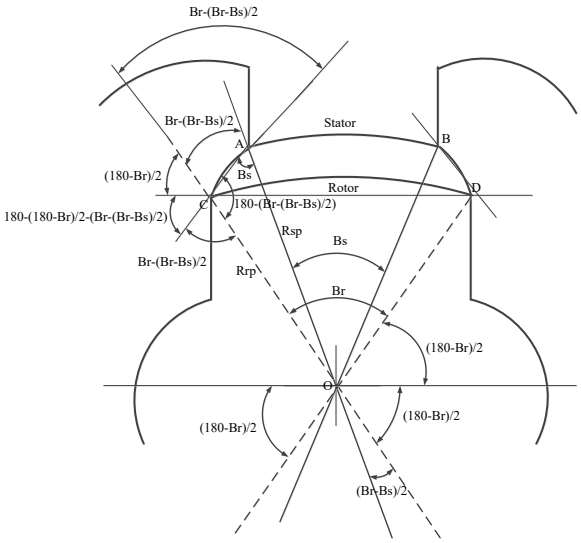


Figure 1. 2/2 DSRM geometric dimensions and the angles when Br > Bs

The triangle ACOA in Figure 2 is obtained from Figure 1

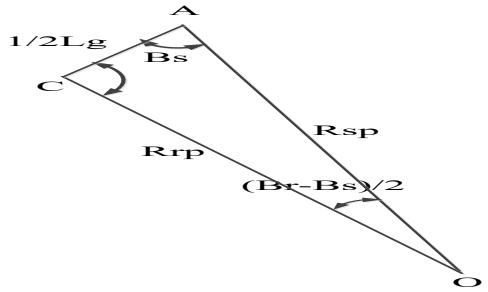


Figure 2. Triangle ACOA

From triangle ACOA:

$$Angle\ ACO = 180 - (Br - \frac{(Br - Bs)}{2}) \text{ and } \quad Angle\ AOC = \frac{(Br - Bs)}{2} \tag{1}$$

Using the sine rule, in triangle ACOA:

$$AC = \frac{1}{2} L_g = \frac{R_{sp} \sin(\frac{B_r - B_s}{2})}{\sin(180 - (B_r - \frac{B_r - B_s}{2}))} \tag{2}$$

where Lg is the air gap length at maximum inductance when both stator and rotor pole are in aligned position, Rsp is the radius of the stator pole, Br is the rotor pole arc and Bs is the stator pole arc in degree

From equation (2), the length of the air gap when both the stator and rotor poles are aligned is given by:

$$L_{g-\max} = \frac{2R_{sp} \sin(\frac{B_r - B_s}{2})}{\sin(180 - (B_r - \frac{B_r - B_s}{2}))} \tag{3}$$

The maximum inductance is expressed as:

$$L_{\max} = \frac{\mu_o {N_{tph}}^2 W_{rp} L_{st}}{l_{g_{-\max}}} = \frac{\mu_o {N_{tph}}^2 W_{rp} L_{st}}{\frac{2R_{sp} \sin(\frac{B_r - B_s}{2})}{\sin(180 - (B_r - \frac{B_r - B_s}{2}))}} \tag{4}$$

where $\mu_o = 4\pi \times 10^{-7} H/m$ is the permeability of free space, $W_{rp}$ is the rotor pole width (mm), $N_{tph}$ is the number of turns per phase and $L_{st}$ is the stack length (mm)

The minimum inductance is expressed as:

$$L_{\min} = \frac{\mu_o {N_{tph}}^2 W_{rp} L_{st}}{l_{g_{-\max}}} = \frac{\mu_o {N_{tph}}^2 W_{rp} L_{st}}{h_{rp} + g} \tag{5}$$

where $h_{rp}$ is the rotor pole height (mm) and $g$ is the air gap between the stator and the rotor (mm)

The DSRM air gap length when the rotor pole width is equal to the stator pole width is shown in Figure 3.

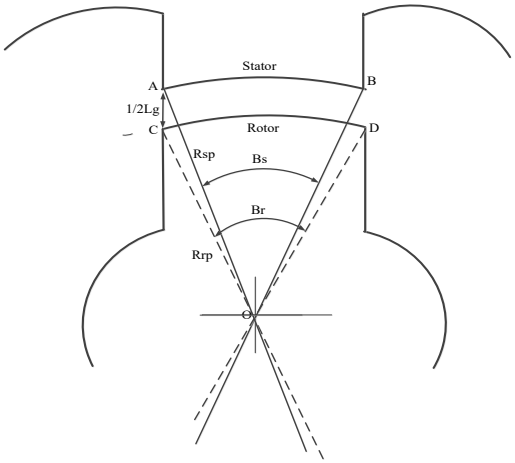


Figure 3. DSRM with stator width equal to the rotor width

The air gap length at maximum inductance when the stator pole width and the rotor pole width are the same is expressed from Figure 3

$$\frac{1}{2}L_g = R_{sp} - R_{rp} = g \; then \; L_g = 2g \tag{6}$$

where $R_{rp}$ is the radius of the rotor pole (mm)

For further investigation on the condition that the stator pole width is larger than the rotor pole width, the air gap length at maximum inductance can be obtained from Figure 4.

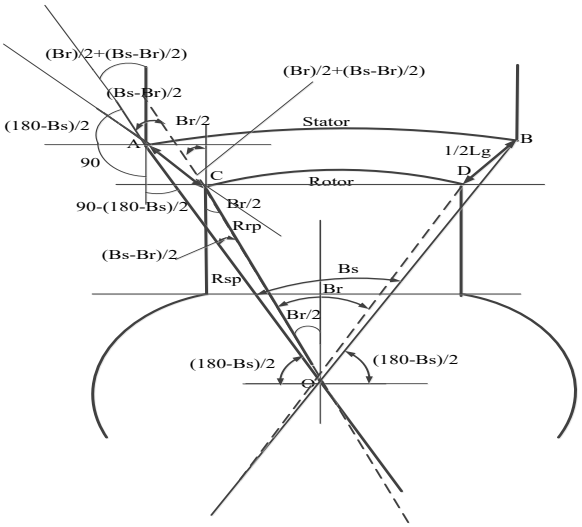


Figure 4. DSRM with stator pole width greater than the rotor pole width

Figure 5 is obtained from Figure 4.

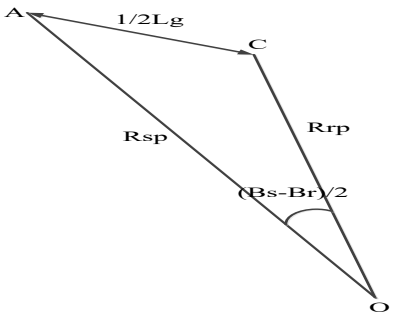


Figure 5. Triangle AOCA

Using the cosine formula:

$$(\frac{1}{2}L_g)^2 = {R_{sp}}^2 + {R_{rp}}^2 - 2R_{sp}R_{rp}\cos(\frac{B_s - B_r}{2}) \tag{7}$$

Equation (7) is re-arranged to make Lg the subject of formula which is the air gap length at maximum inductance

$$L_{g-\max} = 2\sqrt{{R_{sp}}^2 + {R_{rp}}^2 - 2R_{sp}R_{rp}\cos(\frac{B_s - B_r}{2})} \tag{8}$$

The inductance as a function of rotor position is defined as:

$$L(\theta_r) = L_o(1 + m\cos(P_r\theta_r)) \tag{9}$$

where Lo is the average inductance which is half the sum of the maximum and minimum inductance, Ɵr is the rotor position and m is the inductance modulation index. Inductance modulation is defined as:

$$m = \frac{L_{\max} - L_{\min}}{L_{\max} + L_{\min}} \tag{10}$$

The maximum inductance of DSRM with Ps/Pr where Ps is greater than Pr is expressed as:

$$L_{\max} = \frac{P_r\mu_o {N_{tph}}^2 W_{sp} L_{st}}{l_{g_{-\max}}} = \frac{P_r\mu_o {N_{tph}}^2 W_{sp} L_{st}}{\dfrac{2R_{sp}\sin(\frac{B_r - B_s}{2})}{\sin(180 - (B_r - \frac{B_r - B_s}{2}))}} \tag{11}$$

The minimum inductance of DSRM with Ps/Pr where Ps is greater than Pr is expressed as:

$$L_{\min} = \frac{(P_s - P_r)\mu_o {N_{tph}}^2 W_{rp} L_{st}}{l_{g_{-\max}}} = \frac{(P_s - P_r)\mu_o {N_{tph}}^2 W_{rp} L_{st}}{h_{rp} + g} \tag{12}$$

where Ps and Pr are number of stator and rotor poles respectively

**3. Geometric dimensions of DSRM**

*A. Geometric dimensions of 2/2 DSRM*

The geometric dimensions of the 2/2 DSRM are shown in Table 1

Table 1. 2/2 DSRM dimensions

| Symbol | Description | Values |
|---|---|---|
| $D_{os}$ | Outer stator diameter | 194 mm |
| $D_{sp}$ | Diameter of the stator pole (bore diameter) | 100 mm |
| $h_{spn}$ | Stator pole height | 19.07 mm |
| $W_{sy}$ | Stator yoke width (back iron thickness) | 27.92 mm |
| $W_{sp}$ | Stator pole width | 42.26 mm |
| $D_{rp}$ | Diameter of the rotor pole | 99 mm |
| $\beta_s$ | Stator pole arc | 50 degr. |
| $\beta_r$ | Rotor pole arc | 52 degr. |
| $P_r$ | Number of rotor poles | 2 |
| $P_s$ | Number of stator poles | 2 |
| $D_{sh}$ | Shaft diameter | 28 mm |
| $h_{rp}$ | Rotor pole height | 18.05 mm |
| $W_{ry}$ | Rotor yoke width | 17.45 mm |
| $W_{rp}$ | Width of the rotor pole | 43.39 mm |
| $N_{tph}$ | Number of turns per phase | 68 |
| $L_{st}$ | Stack length | 70 mm |

*B. Geometric dimensions of 8/6 DSRM*

Table 2. 8/6 DSRM dimensions [1]

| Symbol | Description | Values |
|---|---|---|
| $\beta_s$ | Stator pole arc | 18 degr. |
| $\beta_r$ | Rotor pole arc | 22 degr. |
| $g$ | Air gap | 0.5 mm |
| $h_{rp}$ | Rotor pole height | 19.8 mm |
| $D_{rp}$ | Diameter of the rotor pole | 100.6 mm |
| $L_{st}$ | Stack length | 200 mm |
| $N_{tph}$ | Number of turns per phase | 154 |
| $P_r$ | Number of rotor poles | 6 |
| $P_s$ | Number of stator poles | 8 |

In order to know whether the developed algorithm can be used to predict other double salient machines with different number of stator and rotor poles, an existing double salient machine whose inductances are known through finite element analysis is investigated. The geometric dimensions of the existing or second machine of 8/6 DSRM are shown in Table 2.

*C. Fabrication of 2/2 DSRM*

The fabricated double salient reluctance machine with a rotor pole and stator pole winding is shown in Figure 6. The rotor position is at 90°.

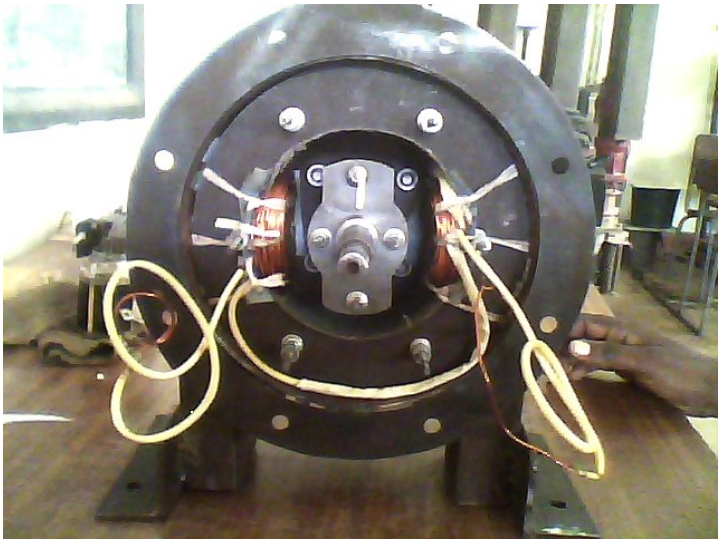

Figure 6. Rotor position at 90 degrees

*D. Simulation result of 2/2 DSRM*

The simulation result of 2/2 DSRM inductance is shown in Figure 7

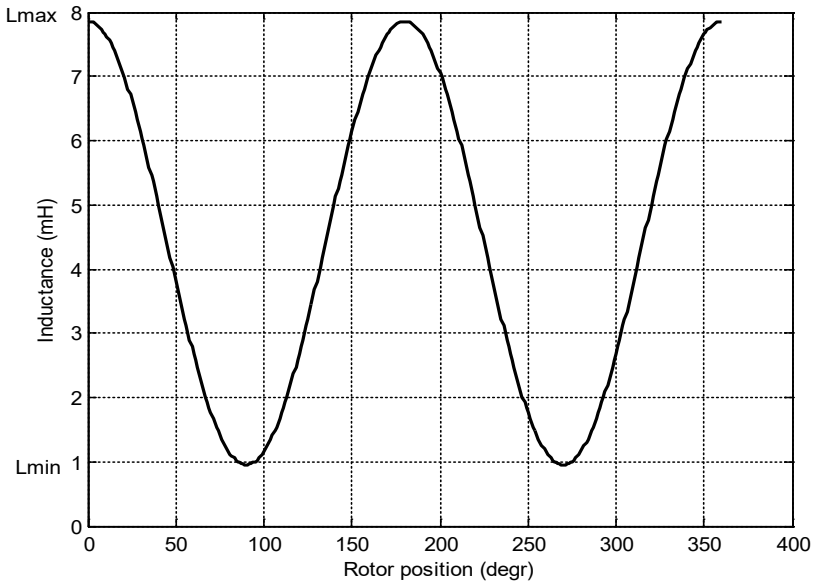


Figure 7. 2/2 DSRM simulation result

## 4. Experimental set up

*A. Experimental set up for inductance measurement*

The experimental set up for inductance measurement with reference to rotor position is shown in Figure 8.

Figure 8. Experimental set up for inductance measurement using LCR meter

*B. Experimental set up of 2/2 DSRM for oscillation*

Figure 9 shows the experimental set up of 2/2 DSRM. The DSRM is coupled with a shunt direct current (dc) motor which acts as a prime mover. The control circuit is then connected to the shunt dc motor. The potential of 2/2 DSRM to sustain oscillation is investigated by connecting oscilloscope to the two terminals of the stator coil. When the control circuit is switched on, the dc shunt motor begins to rotate thereby setting up the 2/2 DSRM into running operation.

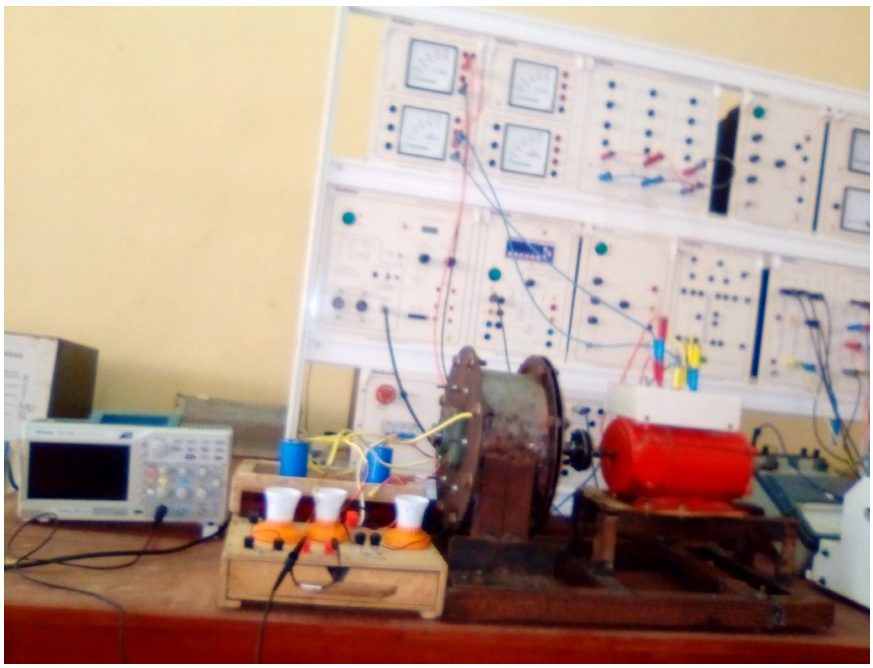

Figure 9. Experimental set up of 2/2 DSRM for sustain of oscillation

**5. Results and discussion**

The experimental results of inductance obtained from the 2/2 DSRM at different rotor positions are shown in Table 3

*Laboratory inductance measurement with reference to rotor positions*

Table 3. 2/2 DSRM Inductance at different rotor position

| Θr (degr.) | L (mH) | Θr (degr.) | L (mH) | Θr (degr.) | L (mH) | Θr (degr.) | L (mH) |
|---|---|---|---|---|---|---|---|
| 0 | 7,89 | 90 | 0.97 | 150 | 3.22 | 250 | 1.08 |
| 15 | 6.68 | 95 | 0.97 | 165 | 5.28 | 255 | 1.02 |
| 30 | 4.58 | 100 | 0.96 | 180 | 7.09 | 270 | 0.98 |
| 45 | 2.79 | 105 | 0.96 | 185 | 7.48 | 285 | 0.97 |
| 60 | 1.19 | 110 | 0.96 | 190 | 7.71 | 300 | 1.09 |
| 65 | 1.09 | 115 | 0.99 | 195 | 7.55 | 315 | 2.69 |
| 70 | 1.04 | 120 | 1.00 | 210 | 6.07 | 330 | 4.87 |
| 75 | 1.01 | 125 | 1.04 | 225 | 4.03 | 345 | 6.49 |
| 80 | 0.99 | 130 | 1.18 | 240 | 1.54 | 360 | 7.89 |
| 85 | 0.98 | 135 | 1.33 | 245 | 1.15 | | |

*Analytical and experimental results of 2/2 DSRM*

The analytical and experimental results of 2/2 DSRM inductance, ratio of maximum inductance to minimum inductance and the difference between the maximum and minimum inductance are compared and shown in Table 4. The air gap length at maximum inductance is 2.24 mm while the air gap length at minimum inductance is 18.55 mm. The experimental and analytical results are in good correlation.

Table 4. 2/2 DSRM inductance and Lmax/Lmin

| | Lmax | Lmin | Lmax/Lmin | Lmax – Lmin |
|---|---|---|---|---|
| Experimental result | 7.86 mH | 0.95 mH | 8.27 | 6.91 mH |
| Analytical result | 7.89 mH | 0.97 mH | 8.13 | 6.92 mH |

*Analytical and Finite Element Analysis of an existing 8/6 DSRM*

The validation of the proposed analytical algorithm for 8/6 DSRM inductances with known results from the finite element analysis (FEA) that are shown in Table 5. The results are in good agreement

Table 5. 8/6 DSRM inductance

| Inductance | Finite Element Analysis | Analytical |
|---|---|---|
| Lmax (mH) | 65.41 | 66.70 |
| Lmin (mH) | 11.35 | 11.27 |

*Inductance profile*

The inductance profile of the 2/2 DSRM at different rotor positions from the experimental data and calculated results are shown in Figure 10. This is the topology of the fabricated 2/2 DSRM inductance profile. The DSRM maximum inductance at 180 degree is slightly different from the analytical due to inaccuracy of the manufacturer during manufacturing process which lead to slightly non-alignment of the shaft and its effect is seen in output waveform. The minimum inductance is observed at 90 and 270 degrees while the maximum inductance is observed at 0 and 360 degrees.

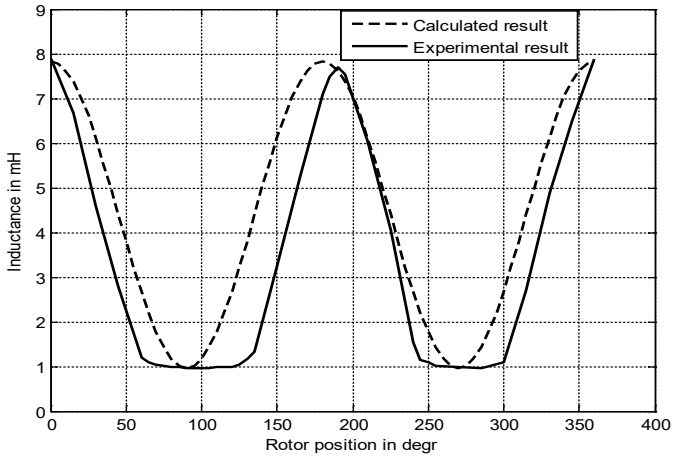


Figure 10. 2/2 DSRM Inductance profile

*Result of the 2/2 DSRM experimental set up*

The oscilloscope displayed induced voltage wave form across the stator coil whose magnitude depends on the speed of the dc shunt motor. When the dc shunt motor speed is 100 rpm, the 2/2 DSRM converted mechanical energy into electrical energy. The inductance voltage at that speed is 30 volts. The machine has the potential to sustain oscillation. This is shown in Figure 11.

Figure 11. Oscilloscope display of inductance voltage wave form across 2/2 DSRM stator coil

*Effect of ratio of maximum to minimum inductance on the differences between the rotor and stator pole arcs*

The ratio of the maximum inductance to the minimum inductance versus the air gap length for different stator and rotor pole arcs of 2/2 DSRM is shown in Figure 12. When the stator and rotor pole arcs are the same, (Br=Bs), the ratio (Lmax/Lmin) is high. The value of air gap length at that point is 1 mm. When the rotor pole arc is greater than the stator pole arc (Br > Bs), the air gap length is 2.4 mm. As the stator pole arc is greater than the rotor pole arc (Bs > Br), the air gap length is 9 mm.

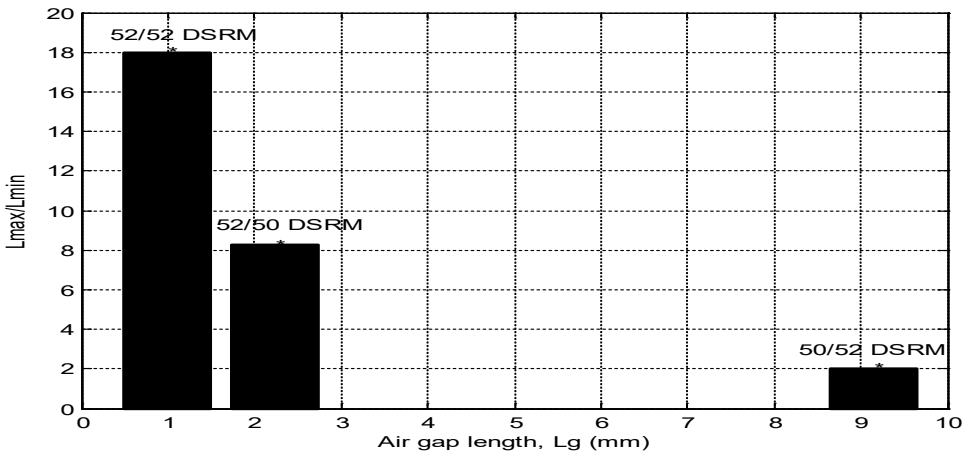


Figure 12. Lmax/Lmin versus Lg-max

Figure 13 shows that the air gap length at maximum inductance depends on the difference between the stator pole arc and the stator pole arc. The greater the change in the stator and rotor pole arcs , the higher is the air gap length.

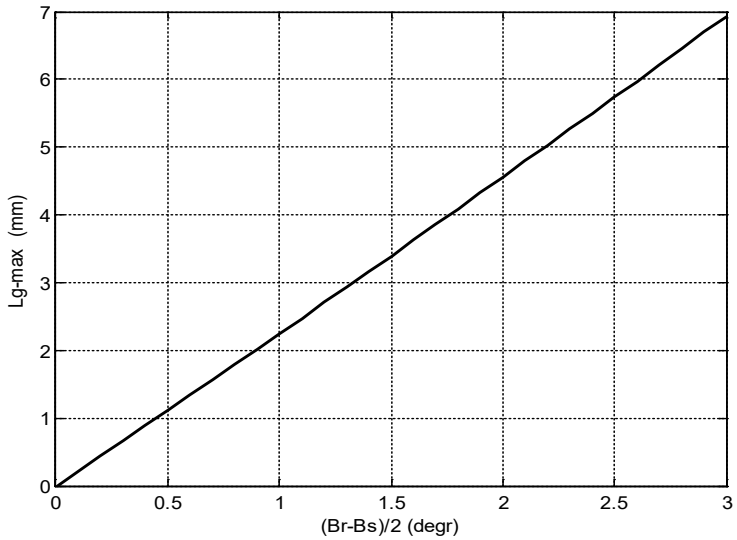


Figure 13. Lg-max versus (Br-Bs)/2 of 2/2 DSRM

As the maximum inductance increases, the air gap length decreases. This is illustrated in Figure 14.

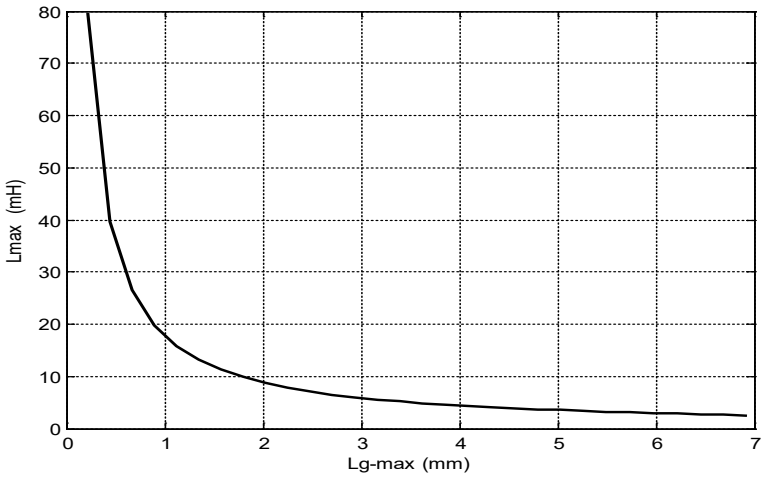


Figure 14. Lmax versus Lg-max

The rotor pitch ratios of the different DSRM configurations versus the rotor pole arcs are shown in Figure 15. A machine with a high pole arc has a low pole-pitch ratio.

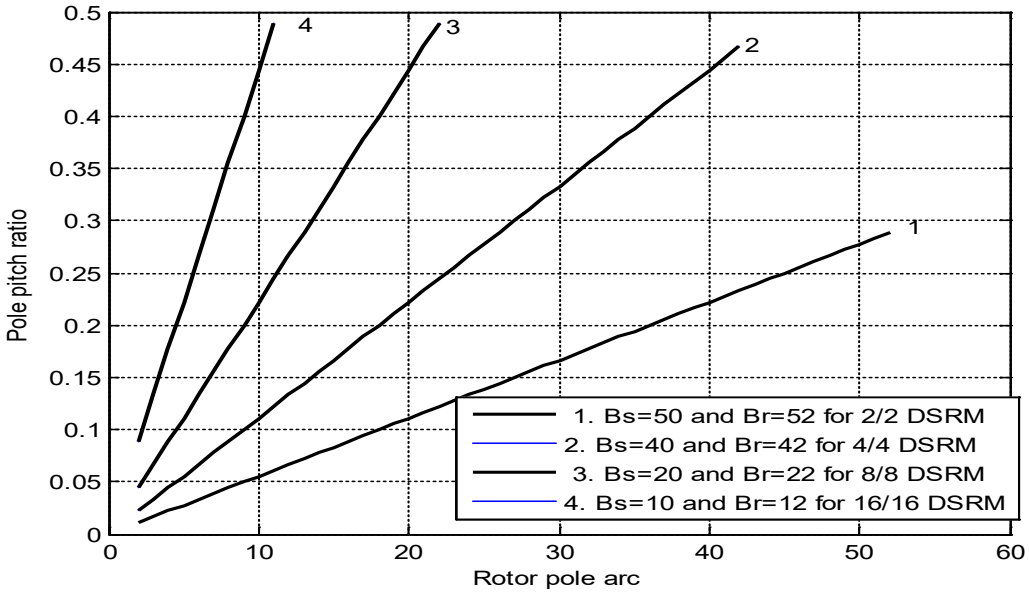


Figure 15. Pole pitch ratio versus rotor pole arc

**6. Conclusion**

The results of the validation of the proposed analytical algorithm developed to predict the air gap length and the maximum and minimum inductance of the double salient reluctance machine are in good agreement with the experimental results. The maximum and minimum inductance of 2/2 DSRM with rotor pole width greater than stator pole width, rotor pole width less than stator pole width and rotor pole width equal to stator pole width are investigated. DSRM with a small difference between the rotor pole arc and the stator pole arc has the potential to produce a high ratio of maximum inductance to minimum inductance To validate the newly developed analytical algorithm, the results of the finite element analysis of the maximum and minimum inductance of an existing 8/6 DSRM is compared with our proposed

analytical method and both are in good correlation. The fabricated 2/2 DSRM configuration has the potential to generate and sustain oscillations.

## 7. Acknowledgments

The first author wishes to appreciate Engineer Mbanu Kingley of Scientific Equipment Development Institute (SEDI), Enugu, Nigeria, who played a major role during the manufacturing process, and Mr. Azu Austine, a tehnologist in an electrical machine workshop at the University of Nigeria, Nsukka, for winding the machine on time without delay.
The last author wishes to acknowledge the support received from the World Bank Africa Centre of Excellence for Sustainable Power and Energy Development (ACE-SPED), University of Nigeria, Nsukka.

## 8. Reference

[1]. R. Krishnan, "Switched reluctance motor drives: Modeling, Simulation, Analysis, Design, and Applications," CRC Press , Boca Rat. London, New York Washington, DC, no. 2nd series, pp. 1.14a-1.14e, 2001
[2]. S. Maruthachalam and N. Palaniswamy, "Determination of Flux linkage Characteristics and Inductance of a Submersible Switched Reluctance Motor using Software Tools," vol. 7, no. 2, pp. 179–187, 2011.
[3]. C. Lee, "Flux linkage estimation in a switched reluctance motor using a simple reluctance circuit," J. Magn., vol. 18, no. 1, pp. 57–64, 2013.
[4]. W. Sriwannarat, A. Siritaratiwat, and P. Khunkitti, "Structural Design of Partitioned Stator Doubly Salient Permanent Magnet Generator for Power Output Improvement," Adv. Mater. Sci. Eng., vol. 2019, no. 1, pp. 1–8, 2019.
[5]. M. N. Anwar, I. Husain and A. V. Radun. A Comprehensive Methodology for Switched Reluctance Machines. *IEEE Trans. Ind.* Appl., 2001, vol. 31, no. No 6, pp. 1684–1692, 2001.
[6]. J. Faiz and J. W. Finch. Aspects of Design Optimization for Switched Reluctance Motors, IEEE Tnransactions Energy Convers, vol. 8, no. 4, pp. 704–713, 1993.
[7]. A. V. Randun. Design Considerations for Switched Reluctance Motor, I*EEE Trans. Ind. Appl.*, vol. 31, no. 5, pp. 1079–1087. 1995.
[8]. R. A. Krishnan, R. Arumugam and J. F, Lindsay. Design Procedure for Switched-Reluctance Motors, IEEE Trans. Ind. Appl., vol. 34, no. 3, pp. 456–461, 1988.
[9]. A. R. Miles, Design of 5MW, 9000V switched reluctance motor, *IEEE Trans. Ind. Appl*., vol. 6, no. 3, pp. 484–491, 1991
[10]. M. A. Aboungem, S. Ali, and D. M. Alzentani, Steady - State Analysis of 6 / 4 Switched Reluctance Motor using Matlab/Simulink Environment, Conf. on Adv. In computer science and electronics engineering, no. 1, pp. 161–166, 2014.
[11]. A. Arifin, "State of the Art of Switched Reluctance Generator," *Energy Power Eng.*, vol. 10, no. 4r, pp. 447–458, 2012
[12]. M. Nassereddine, "Switched Reluctance Generator for Wind Power Applications," *Sch. Eng. Univ. West. Sydney*, pp. 1–131, 2011.
[13]. D. Susistra, A. E. Jebaseeli "Switched Reluctance Generator- Modeling, Design, Simulation, Analysis and Contol A Comrehensive Review," Int. *J. of Computer Applications.* Vol. 1, No.2, pp. 10-16.
[14]. E. A. Anazia, K. C. Obute, O. Oduyemi, and E. C. Eze, "Imperatives of Air-Gap Length on the Performanceof Electromechanical Devices / Machines Imperatives of Air-Gap Length on the Performance of Electromechanical Devices / Machines," *IOSR J. Electr. Electron. Eng.*, vol. 15, no. 3, pp. 15–23, 2020.
[15]. Y. Benômar, J. Croonen, B. Verrelst, J. Van Mierlo, and O. Hegazy, "On analytical modeling of the air gap field modulation in the brushless doubly fed reluctance machine," *Energies*, vol. 14, no. 9, pp. 1–25, 2021.

[16]. R. R. Kumar, S. K. Singh, R. K. Srivastava, and R. K. Saket, "Dynamic reluctance air gap modeling and experimental evaluation of electromagnetic characteristics of five-phase permanent magnet synchronous generator for wind power application," *Ain Shams Eng. J.*, vol. 11, no. 2, pp. 377–387, 2020.
[17]. Y. Yang, R. Wang, and X. Zhu, "Suspension principle and verification of 6/4 pole bearingless switched reluctance motor with permanent magnets in its stator yoke," *AIP Adv.*, vol. 11, no. 11, p. 115106, 2021.
[18]. A. Judge, "Air-Gap Elimination in Permanent Magnet Machines," *Worcester Polytech. Inst.*, pp. 1–175, 2012.
[19]. W. S. Yao, "Rapid optimization of double-stators switched reluctance motor with equivalent magnetic circuit," *Energies*, vol. 10, no. 10, 2017.
[20]. M. Wallin *et al.*, *Measurement and modelling of unbalanced magnetic pull in hydropower generators*. 2013.
[21]. M. Ezzat, "Winding Function Analysis Technique as an Efficient Method for Electromagnetic Inductance Calculation," *J. Electr. Eng.*, pp. 1–5.
[22]. E. S. Obe, "Calculation of inductances and torque of an axially laminated synchronous reluctance motor," *IET Electr. Power Appl.*, vol. 4, no. 9, p. 783, 2010.
[23]. T. Lubin, T. Hamiti, H. Razik, and A. Rezzoug, "Comparison between finite-element analysis and winding function theory for inductances and torque calculation of a synchronous reluctance machine," *IEEE Trans. Magn.*, vol. 43, no. 8, pp. 3406–3410, 2007.
[24]. I. K. Onwuka and U. U. Uma, "Determination of The Winding Inductances Of A Two-Phase," *IOSR J. Eng.*, vol. 5, no. 4, pp. 16–22, 2015.
[25]. M. B. Rego, L. C. Gomes, A. B. F. Neves, A. W. F. V Silveira, and E. A. A. Coelho, "Survey of Inductance Curves in Switched Reluctance Machines Using Finite Elements Key words," pp. 1–5, 2012.

**Yahaya ENESI** was born on June 26, 1964, in the Okenne Local Government Area of Kogi State, Nigeria. He received his M.Sc. from Zaporozhye State Technical University, Republic of Ukraine in 1995. He lectures in the electrical engineering department at Federal University of Technology, Minna. He is currently pursuing his Ph.D. at University of Nigeria, Nsukka. His research interests include electrical machines and parametric oscillations

**Ajah VICTOR** was born 22nd February 1984, in Ishinagu Ebonyi state. He received his Master in Engineering from University of Nigeria, Nsukka in 2018. His research areas include control systems, power electronics and renewable energy.

**Emenike C. Ejiogu** was educated at the University of Nigeria, Nsukka for B. Eng (1987) and 1990 (M.Eng.), before proceeding for his PhD studies from 1990 to 1994 at the National Shinshu University, Nagano-city, Japan. He has held various positions in the academia and industrial sector from 1994 till present, in Japan. In addition, in 2011 he was appointed a professor at the University of Nigeria, Nsukka. He has numerous publications in international conferences and journals. He also has international patents in new energy systems. His areas of expertise include industrial electronics, power devices and new energy systems.